J. Astrophys. Astr. (1982) **3,** 69–77

Doppler Shift Measurements on the Green Coronal Line—Evidence for Largescale Macroscopic Mass Motion

J. N. Desai and T. Chandrasekhar *Physical Research Laboratory, Ahmedabad 380009*
P. D. Angreji *The Vedhshala, Ahmedabad 380013*

Received 1981 August 24; accepted 1982 February 22

Abstract. Fabry-Perot interferometric observations on the green coronal line (λ 5303 Å) carried out during the total solar eclipse of 1980 February 16 have yielded relative Doppler shift velocities with an accuracy of ± 7 km s^{-1}. The values show a peak in the 30–50 km s^{-1} range indicating largescale macroscopic mass motion in the solar maximum corona.

Key words: total solar eclipse—green coronal line—Doppler shifts

1. Introduction

Doppler shift measurements provide significant observational data on the macroscopic mass motion in the corona. However, coronal-line observations are inherently difficult to make. The data available till recently was limited to a few spectrograms taken sporadically at mountain top coronagraphs and during the brief moments of totality of a few eclipses. These observations—Dollfus (1957) and Billings (1963)—sample only a small portion of the corona as defined by the slit of the spectrograph. Further coronagraphic observations of this type are constrained by scattering effects in the terrestrial atmosphere and rarely go up to 1·2 $R_{\odot}$. The analyses of the spectro grams have not yielded any significant Doppler shift in the coronal lines.

More recently, Fabry-Perot interferometric observations in the green coronal line (λ 5303 Å) and the red coronal line (λ 6374 Å) have been attempted from which it is possible in principle to determine Doppler shifts at many different points in the corona simultaneously (Liebenberg 1975; Delone and Makarova 1969; Hirschberg, Wouters and Hazelton 1971). Liebenberg (1975), discussing the results of the eclipse of 1965 May 30, finds Doppler shifts in the green line to be < 5 km s^{-1}. Delone and Makarova (1969), after a study of 170 profiles of the red line and 20 profiles of the green line, however find significant Doppler velocities in the range 10–40 km s^{-1}

during the same eclipse. In some active regions their values go up to 70 km s^{-1}. Hirschberg, Wouters and Hazelton (1971) have reported a complex vortex structure with green-line Doppler-shift velocities of ∼ 6 km s_{-1} from their observations of the 1970 eclipse. Harvey and Livingston (1981) reporting the observations taken with a multi-slit high-dispersion spectrograph during the 1980 eclipse find in 30 per cent of their samples inward flow velocities in the range 3–15 km s^{-1}

We present in this paper results indicating significant Doppler shifts in the green line in the velocity range 30–50 km s^{-1} from the interferometric observations made during the total solar eclipse of February 16, 1980 at Gadag, India (15° 25′ N, 75° 37′ E).

2. Instrumentation

Fig. 1 is a schematic sketch of the experimental set up used during the eclipse. Coronal light, after reflection from the coelostat mirror M, was collected by an achromatic lens O (focal length 2280 mm; f/15 system) to form the image at focal position A. An interference pre-filter centred at λ 5303 Å with a bandwidth of 7 Å F isolated the green line. After 'A' the light was recollimated by the lens L_1 (focal length 80 mm; f/1·2 system), allowed to pass through the Fabry-Perot etalon E and finally imaged by a camera lens L_2 (focal length 55 mm; f/1·2 system) on the 35 mm film format C. Precalibrated (step wedge calibration supplied by Kodak) Kodak (400 ASA) 35 mm film was used.

The Fabry-Perot etalon E was an optically-contacted one which ensured complete freedom from misalignment problems which usually plague Fabry-Perot systems. The etalon had an air-spacing of 307 μm, a coating of 88 per cent reflectivity at λ 5303 Å and a free spectral range of 4·7 Å at λ 5303 Å. The finesse value was ∼ 20.

In order to evaluate the system performance, immediately after totality the interferometer was calibrated using a spectral lamp in the green line of mercury (λ 5460·74 Å). Microdensitometry of this calibration frame yielded an instrumental profile of full width at half-maximum (FWHM) ∼ 0·23 Å. The shape of this profile is shown along with the theoretical Airy and Gaussian profiles of the same FWHM (Fig. 2). The instrumental line shape is seen to follow the Airy profile closely indicating that the Fabry-Perot etalon had been in excellent alignment during the period of totality.

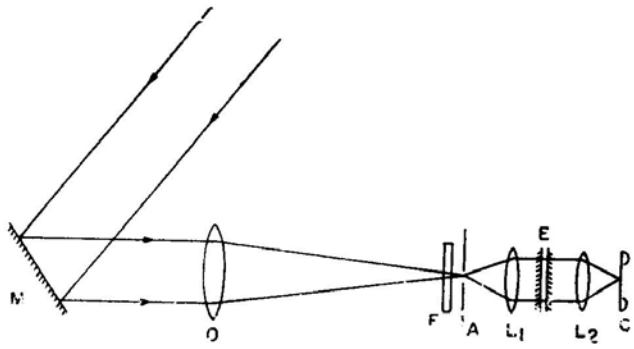

Figure 1. Experimental set up.

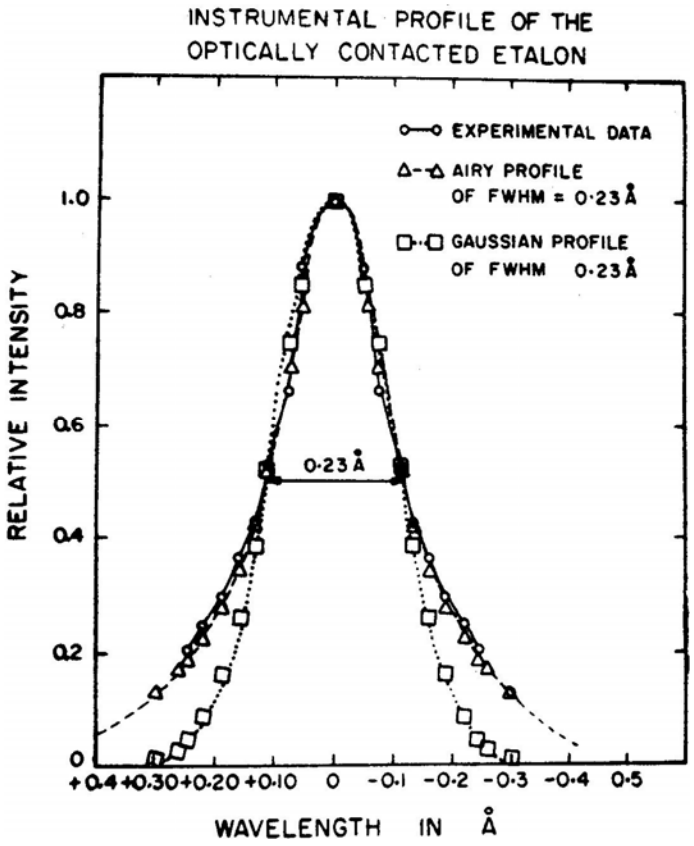

Figure 2. Instrumental profile.

3. Observations and redaction procedure

Four photographs were taken under perfect sky conditions during the 2 min 46 s of totality with exposure times 4, 10, 30 and 90s. All exposures recorded the interferogram successfully. The 90s frame is shown in Fig. 3.

The centre of the Fabry-Perot system was kept off-centred with respect to the centre of the solar disk by $\sim$ 20 arcmin. This was done to ensure continuous measurements of FWHM along a few position angles. However, about 1/3 of the azimuthal coverage had to be sacrificed to gain this advantage. Hence no fringes are seen between position angles 95° and 220°. The order of interference ranges from 1130 to 1150.

The eclipse frames along with the mercury line calibration frames were simultaneously developed strictly according to the specifications of the manufacturer. All the frames were then scanned on a Carl Zeiss microdensitometer with a slit area corresponding to 13 arcsec × 6 arcsec in the plane of the sky. From the densitometry of the wedge calibration, the photographic curve was constructed, digitised and used in the calculation of relative intensities. On the eclipse frames microdensitometric scans were made radially outwards from the fringe centre, Since the green

line during this eclipse was much stronger than the continuum in the 7 Å bandwidth filter used, $\left(\frac{E_{\text{line}}}{E_{\text{continuum}}} > 10\right)$ the fringes had a high contrast and there was no ambiguity in locating the fringe peaks. Fringes are observed from 0·03 $R_\odot$ above the solar limb upto 0·5 $R_\odot$. Typically, fringe peaks could be located with an accuracy of ± 0·05 mm on the film as measured from the fringe centre. The fringe peaks could however be located with respect to each other with a much greater accuracy of < ± 0·005 mm. This value translates to a relative line of sight velocity of ± 6 km s^{-1}. Any shift in the centre of the fringe pattern between the eclipse frame and the calibration frame can significantly affect absolute Doppler velocity determination. Since relative fringe peak positions can be determined better (< ± 0·005 mm) than their absolute position from the fringe centre (~ ± 0·05 mm) we have considered only the relative Doppler shifts and their standard deviation for each scan. For each scan we calculate the standard deviation of the Doppler shift velocities of the fringes in that scan. Thus, from an examination of 659 fringes spread over 59 scans made radially outwards from fringe centre in the 90 s and 30 s frames we get 59 velocity dispersion values which should be accurate to ± 6 km s^{-1}. In order to verify this expectation we have rescanned the calibration frame treating it as a hypothetical eclipse frame in λ 5461 Å. The dispersion value of ± 7 km s^{-1} obtained agrees very well with calculated error and justifies the method for detecting relative Doppler shifts greater than 7 km s^{-1}. Since each scan is made radially outwards from the fringe centre which has been kept displaced from the solar centre, the dispersion velocity is necessarily averaged over the few degrees of position angle and also over the entire radial extent of the scan. Hence, from this reduction it is not possible to draw any conclusion regarding the radial variation of the dispersion velocity.

The spatial resolution as determined by fringe separation is variable, improving with increasing distance from fringe centre. A typical fringe separation of ~ 0·2 mm on film gives a spatial resolution of 0·03 $R_\odot$ at the corona.

The spacer value (μt) of the interferometer required in the calculations for Doppler shifts was experimentally determined from a careful study of the calibration frame. For this purpose a special projection technique was developed and used by which the frame could be magnified by ~ 200 times. Measurements on the calibration fringes yielded a spacer value of 307 μm with an estimated error of < 1 per cent.

4. Calculation of Doppler shifts

The basic Fabry-Perot equation is

$$2\ \mu t \cos\theta = n\lambda \tag{1}$$

where μt = air-spacer = 307 μm, n = order of interference, λ = wavelength of light and θ is given by

$$\tan\theta = R / F.$$

R refers to the fringe radius (measured from the fringe centre and *not* the solar centre).

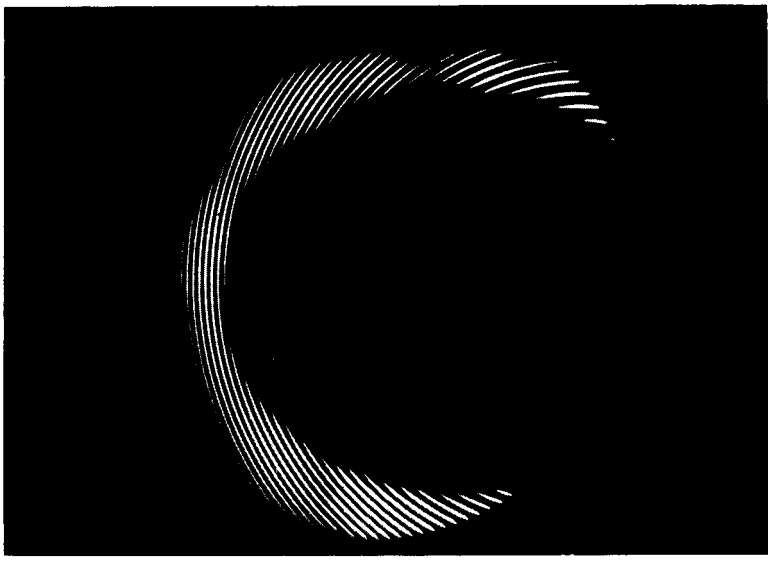

Figure 3. Coronal Interferogram (90s exposure).

F is the focal length of the camera lens used. In our case, F = 55 mm. We have taken the ' rest ' wavelength of the green line to be λ_0 = 5302·86 Å (Unsöld 1977). For the rest wavelength, fringe peak positions are given by

$$2\ \mu t \cos\theta_0 = n\lambda_0. \tag{2}$$

θ_0 can be calculated for the different orders of interference expected in the fringe pattern. Hence

$$2\ \mu t\ (\cos\theta - \cos\theta_0) = n\ (\lambda - \lambda_0)$$

and

$$\frac{\cos\theta - \cos\theta_0}{\cos\theta_0} = \frac{\lambda - \lambda_0}{\lambda_0} = \frac{V}{c}. \tag{3}$$

Measuring R and using calculated θ_0, the line of sight Doppler shift velocity V can be calculated. The standard deviation in V in each densitometric scan is the value actually used in drawing our conclusions.

5. Results

Our results are shown in Figs 4 and 5. Fig. 4 shows standard deviation of the Doppler shift velocities in km s^{-1}—indicated by numbers—plotted for each of the 59 scans in the different portions of the corona. The radial extent of each scan is also marked by a radial line at the mean position angle for the scan. Fig. 5 is a histogram plot of the dispersion velocities deduced from both 90 s and 30 s frames.

6. Discussion

The histogram plotted to bring out the distribution of relative line of sight velocities shows a peak in the velocity range 30–50 km s^{-1}. There is a smaller peak in the histogram in the velocity range 11–20 km s^{-1}.

As seen in Fig. 4 the large dispersion velocities are not confined to a small portion of the corona but apply over a wide range of azimuth and radial extent. Our measurements, further, are not directly measured Doppler shifts but statistically inferred dispersion velocities. They also, by the very nature of their deduction, have the disadvantage of not showing any radial variation in their values. However, as the dispersion velocities measured are significantly above the error limits that we can ascribe to them (~ 7 km s^{-1}), we feel justified in presenting the results.

While linewidth measurements are a measure of thermal and statistically random motion, the dispersion velocities represent the net nonrandom motion directed towards or away from the observer.

There is a considerable body of evidence showing largescale relative motion in the corona above the western limb during this eclipse. Liebenberg and Keller (1980)

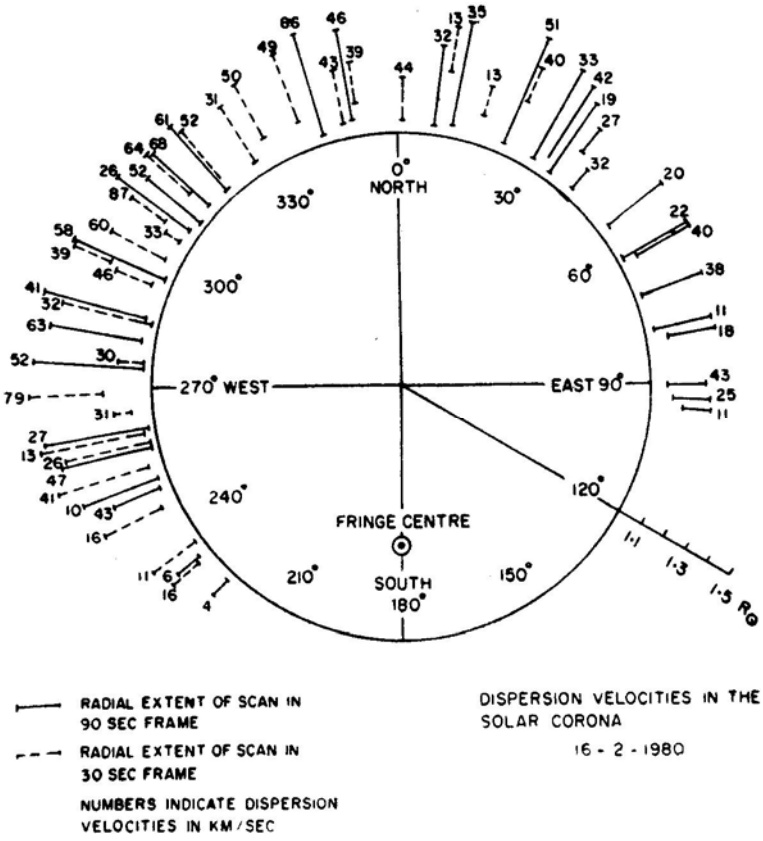

Figure 4. Doppler shift dispersion velocity distribution in the corona.

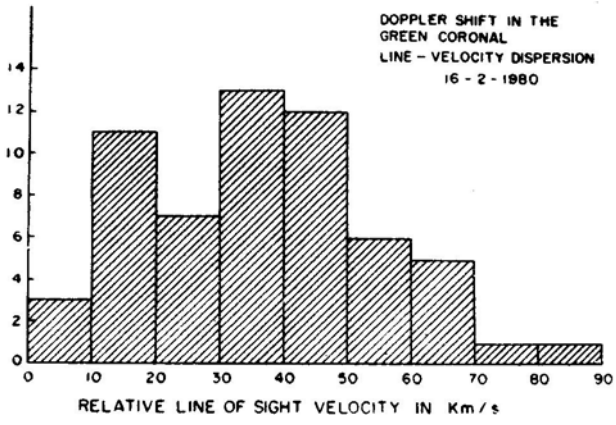

Figure 5. Doppler shift dispersion velocity histogram.

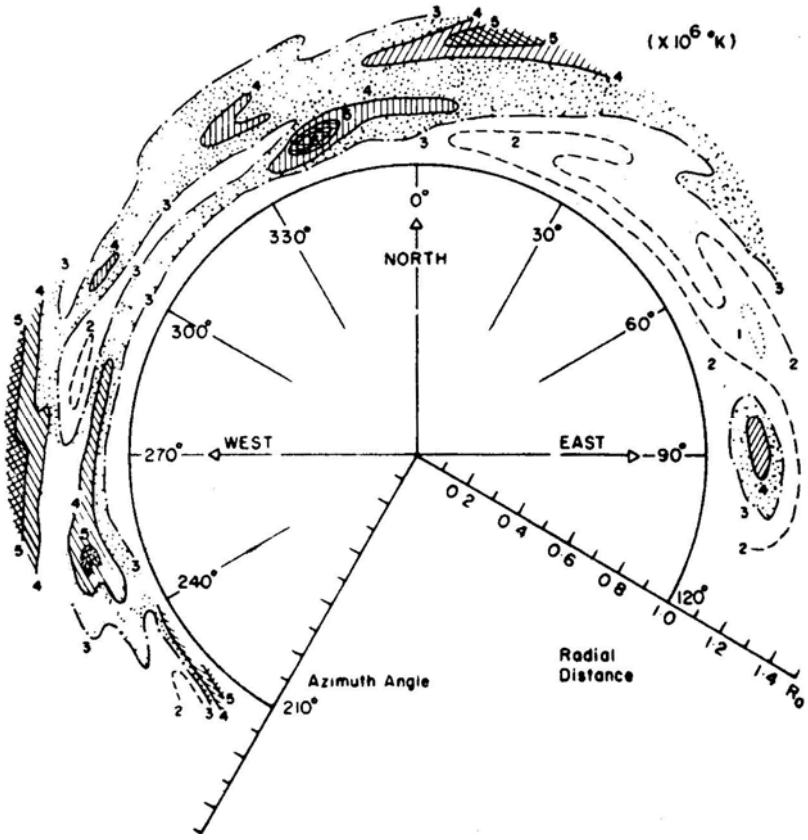

Figure 6. Temperature distribution in the corona.

report a largescale eruptive disturbance in this limb from their aircraft observations. It is also seen in white light pictures taken from Kenya but not in those taken from India 90 min later. Their preliminary results show large streaming velocities in this region. White light coronagraph pictures taken from PS 78–1 satellite a few hours before totality over India, also show mass ejection a few degrees north of west above the solar limb (Koomen 1981, personal communication). In our 30 s interferogram frame, fringe splitting is clearly evident at position angle 256°. The splitting corresponds to a differential mass motion with velocity of $\sim$ 70 $\pm$ 5 km s$_{-1}$ (Chandrasekhar, Desai and Angreji 1981).

Figs 6 and 7 which show the Doppler line-width temperature distribution and the relative intensity distribution of the corona as deduced from the 90 s frame are included mainly for the sake of comparison. It is however difficult to establish one-to-one correspondence between the intensity, temperature and velocity maps. There is a spot of high temperature at position angle 255° and the relative intensity values are also high in the same region. However, Fig. 4 shows nothing unusual in this region. On the other hand, though temperature and intensity show no peculiarities near 315°, the dispersion velocities (Fig. 4) show a consistently high value > 60 km s^{-1} in this portion of the corona. While the fringe-split region may not be linked with the eruptive disturbance, this high value could well be due to the same eruptive distur-

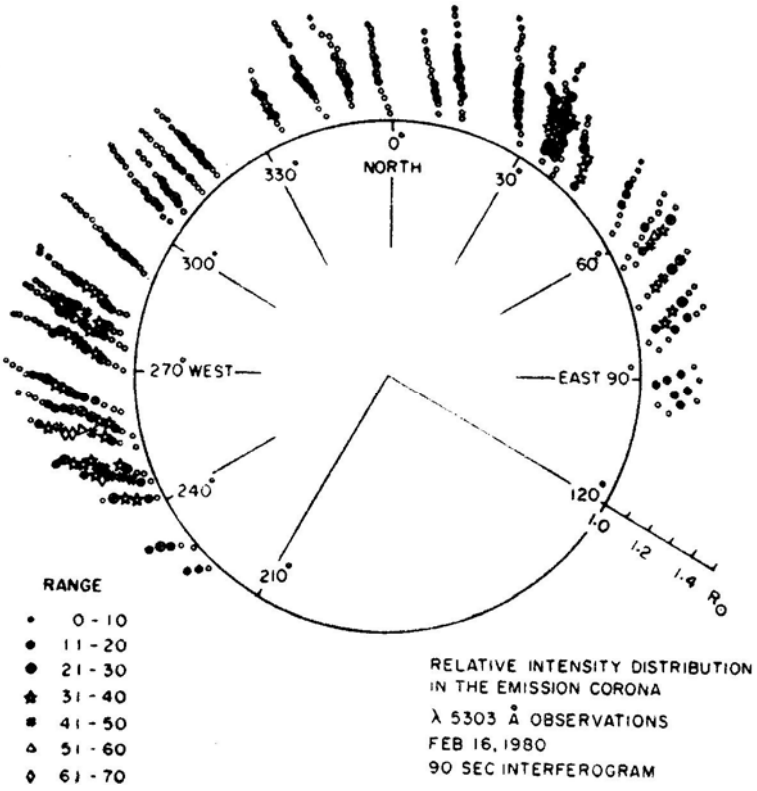

Figure 7. Relative intensity distribution in the corona.

bance mentioned earlier. Dispersion velocities are not low in other parts of the corona too suggesting largescale relative motion in the solar maximum corona.

7. Conclusion

Relative Doppler shift measurements in the green coronal line have yielded values mainly in the range 30–50 km s^{-1}. The measurements spread over a large portion of the corona in azimuth and upto 1·5 $R_\odot$ in radial extent indicate largescale macroscopic mass motion in the solar maximum corona.

Acknowledgements

The authors wish to thank J. Pasachoff of Hopkins Observatory, Massachusetts for a timely supply of precalibrated films. The authors are also grateful to M. J. Koomen of Naval Research Laboratory, Washington, D. C. for the preliminary unpublished white light coronagraphic data obtained by PS 78–1 satellite. The work was financially supported by Department of Space, Government of India.

References

Billings, D. E. 1963, *Astrophys. J.,* **137,** 592.
Chandrasekhar, T., Desai, J. N., Angreji, P. D. 1981, *Appl. Opt.,* **20,** 2172.
Delone, A. B., Makarova, E. A. 1969, *Solar Phys.,* **9,** 116.
Dollfus, A. 1957, *C.r. hebd. Seanc. Acad. Sci. Paris,* **244,** 1880.
Harvey, J., Livingston, W. 1981, in *Proc. International Symposium on Solar Eclipse,* INSA, New Delhi.
Hirschberg, J. G., Wouters, A., Hazelton, L., Jr. 1971, *Solar Phys.,* **21,** 448.
Liebenberg, D. H. 1975, *Solar Phys.,* **44,** 331.
Liebenberg, D. H., Keller, C. F. 1980, *Los Alamos Science,* p. 1.
Unsold, A. 1977, *The New Cosmos,* 2 edn, Springer-Verlag, New York, p. 191.